Tunable Generation and Angular Steering of a Millimeter-Wave Orbital-Angular-Momentum Beam using Differential Time Delays in a Circular Antenna Array

Guodong Xie[1,*], Yan Yan[1], Zhe Zhao[1], Long Li[1], Yongxiong Ren[1], Nisar Ahmed[1], Asher J. Willner[1], Changjing Bao[1], Zhe Wang[1], Cong Liu[1], Nima Ashrafi[2,3], Solyman Ashrafi[2], Shilpa Talwar[4], Soji Sajuyigbe[4], Moshe Tur[5], Andreas F. Molisch[1], and Alan E. Willner[1]

1. Department of Electrical Engineering, University of Southern California, Los Angeles, CA 90089, USA
2. NxGen Partners, Dallas, TX 75219, USA
3. University of Texas at Dallas, Richardson, TX 75080, USA
4. Intel Labs, Intel Corporation, Santa Clara, CA 95054, USA
5. School of Electrical Engineering, Tel Aviv University, Ramat Aviv 69978, Israel
Corresponding email*: guodongx@usc.edu

Abstract— **In this paper, the generation and steering of beams carrying orbital angular momentum utilizing a custom-designed circular antenna array has been demonstrated at 28 GHz. A steering angle as large as 30 degrees for an orbital angular momentum (OAM) beam has been achieved. The effect of number of antennas and the distance from antennas to the array center to the quality of beam generation and beam steering is investigated through both experiments and simulations. Our results indicate that: (1) As the steering angle increases, the mode purity of the generated OAM beams decreases; (2) Increasing the number of antennas improves the OAM mode purity; (3) For a fixed number of antennas, high mode purity is observed for lower order OAM modes; (4) Placing the antennas farther away from the array center allows for reduced divergence of the generate OAM beams.**

Keywords— Orbital angular momentum; Beam steering; Mode purity.

I. INTRODUCTION

Spectrum is precious in free-space RF line-of-sight (LoS) communication links, there is a continual need to increase both the capacity and spectral efficiency of such systems [1]. One approach for such an increase is by transmitting multiple orthogonal data-carrying beams through a single transmitter/receiver aperture pair [2-4]. If each beam occupies a unique mode in an orthogonal basis set, then efficient multiplexing and transmission can occur with little inherent crosstalk and mode mixing. Such mode-division-multiplexing, which is a subset of space-division-multiplexing [5], has been demonstrated (or discussed) in millimeter, microwave, and optical regions for free-space LoS communication links using multiple orbital-angular-momentum (OAM) modes [2-4, 6-15].

OAM is commonly manifested by a beam's phase front "twisting" in a helical fashion as it propagates. The beam's OAM value is the number of 2π phase shifts that occur in the azimuthal direction, and an OAM beam typically has a ring-intensity with a central null. Each of multiple data-carrying OAM beams can have a unique OAM value, and the orthogonal beams spatially overlap during propagation [16,17].

OAM can be generated in several ways, including: (i) passing a conventional Gaussian beam though a phase hologram such as a spiral phase plate [4,18,19], and (ii) directly generating an OAM beam from a circular array of emitting antenna elements [20-22]. An antenna array can be compact in size, multiple arrays can be concentrically stacked one on top of another for generating multiple OAM beams, and the array can generate different OAM values by adjusting the relative time/phase delay introduced to each element [20].

One key issue for many OAM-based multiplexed links is the accurate alignment of the transmitter aperture with the receiver aperture [23]. If multiple OAM beams are transmitted, the receiver must be able to distinguish one beam from another and determine what OAM mode value exists. This can be accomplished by ensuring that the beam center hits the receiver aperture center, since the central region has the most phase change per unit area [16,17]. Deviation off center will cause power at the receiver to be coupled into other modes [23]. Therefore, a laudable goal for an OAM-based communications link would be the ability to steer the transmitted beam such that it hits the receiver at the appropriate spot. There has been little reported on steering of an OAM beam.

I n this paper, we demonstrate tunable generation and angular steering of a millimeter-wave OAM beam using differential time delays in a circular antenna array [20-23]. Similar to conventional antenna arrays, beam steering can be achieved by adding relative phase delays among antennas in the steering directon to tilt the beam. At the same time, OAM generation could be achieved by applying relative phase delays in the azimuthal direction. By tailoring the relative time delays among anttennas, we simultaneously generate and steer an OAM beam with a steering angle as large as 30°. The effect of antenna number and the distance from antennas to the array center to the quality of the OAM generation and beam steering is also investigated through experiments and simulations.

II. CONCEPT AND EXPERIMENTAL DESIGN

A. Concept of the generation and steering of beams carrying OAM utilizing a custom-designed circular antenna array

The concept of using a circular antenna array for the generation and steering of beams carrying OAM is shown in Fig. 1. A millimeter-wave signal is split into N branches (the

case of N=8 is shown in Fig. 1). Each branch has a tunable delay line (TDL) followed by an antenna. The TDLs are used to control the relative phase delays among different branches. The antennas are circularly arranged such that each antenna has the same distance to the center of the array. Such a custom-designed circular antenna array obeys following criteria:

- An OAM beam has a spiral phase front varying from 0 to $2\ell\pi$. Therefore, by tuning phase delays among the circularly arranged antennas from 0 to $2\ell\pi$ according to their azimuthal angles (Fig. 1 (a)), an OAM+ℓ beam could be generated.
- The propagation direction of a beam is always perpendicular to its equiphase surface. Therefore, by tuning the phase delays among the antennas according to their positions in the steering direction (Fig. 1 (b)), the generated beam would propagate at an angle.
- When the phase delays among the antennas are the sum-up of the phase delays in the above two criteria, the beam steering and OAM+l beam generation could be done simultaneously.

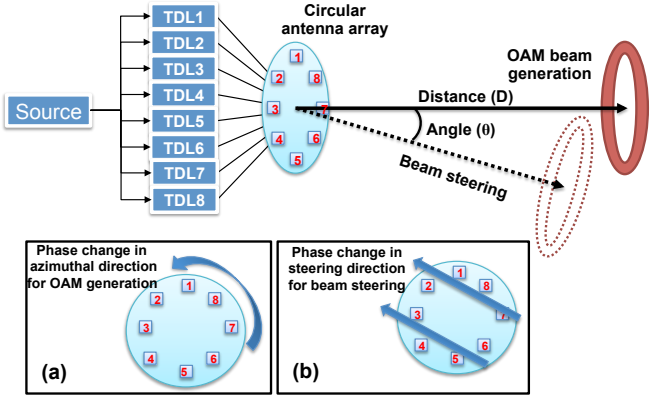

Figure 1. Concept of using circular antenna array for the generation and steering of beams carrying OAM. TDL: tunable delay line. (a) Phase change in the azimuthal direction for OAM generation. (b) Phase change in the steering direction for beam steering.

B. Experimental design of using circular antenna array for the generation and steering of beams carrying OAM

In the proposed approach, precise control of the phase delay for each branch and accurate antenna arrangement are essential for the quality of the OAM beam generation and steering. The following approaches are employed to guarantee the performance of the system.

Figures 2 (a) and 2(b) show the designed tunable delay line array for phase delay control and arrangement of the antennas. For our experiment, we use N = 8. Each of the eight branches is connected to an individual "trombone-like" tunable delay line before being connected to an antenna. To precisely measure the phase delay among branches, a probe receiver is designed that could collect the millimeter-wave right after an antenna on the circular array (Fig. 2(c)). The collected millimeter-wave is then sent to an oscilloscope to compare its relative phase with a reference signal. Keeping the probe receiver, the cable, and the reference signal the same, this measurement could be repeated for all the branches one after another. Therefore, the relative phase delays among all antennas could be measured.

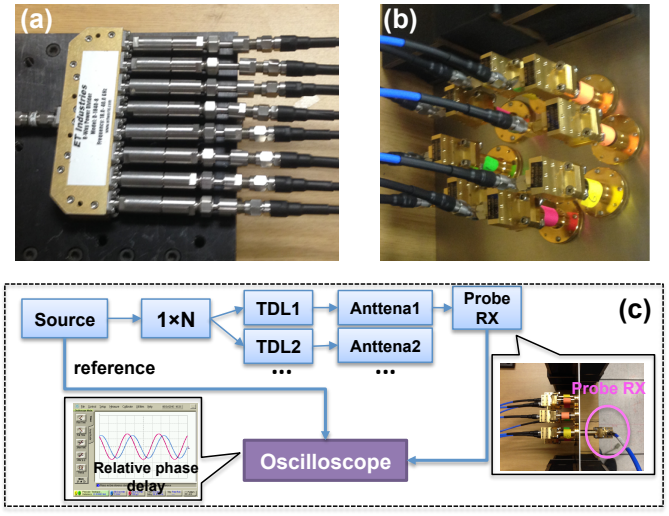

Figure 2. Design of (a) the tunable delay line array and (b) the arrangement of antennas. (c) The approach for tuning and measuring the relative phase delays among different branches.

The design of the circular antenna array and its appearance are shown in Fig. 3. The eight antennas, each of which has the radius of r, are placed on a circle of radius R. To fix the antennas, eight holes are drilled in an aluminous breadboard, using a computer-numerical-control (CNC) machine. For our experiment, we developed three breadboards having R = 4.5 cm, 5.0 cm and 6.0 cm. The radii r of each antenna are 2.1 mm.

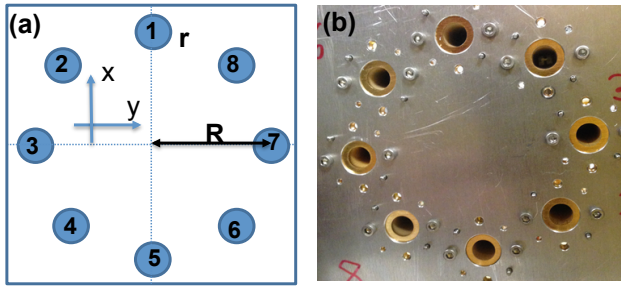

Figure 3. (a) Arrangement and design parameters of the circular antenna array. (b) The appearance of the designed breadboard to hold the antennas. x and y directions are defined here and will be used in the discussion afterwards.

III. OAM Generation Using Circular Antenna Array

To generate a spiral phase, the relative phase delays of the eight antennas are tuned to be: 0, $\pi/8$, $\pi/4$, $3\pi/8$, $\pi/2$, $5\pi/8$, $3\pi/4$, $7\pi/8$, respectively. The intensity profiles of the generated beams are captured via a probe antenna with a small aperture of radius ~2 mm. The output of this probe antenna is recorded by an RF spectrum analyzer. The probe antenna is placed on a two-dimensional (2D) linear translation stage with a scanning step of 1.5 cm and a transversal coverage area of 48 cm × 48 cm. Figure 4 depicts the numerically calculated and experimentally measured intensity profiles of the generated OAM+1 beams at various distances ranging from 0.4 m to 1.2 m. As the beam propagates in free space, it diverges and the ring-shape becomes clearer. As can be seen in these figures, our measurements agree well with the numerical calculations.

The coarseness of the measured intensity profiles is due to limited resolution of the 2D stage.

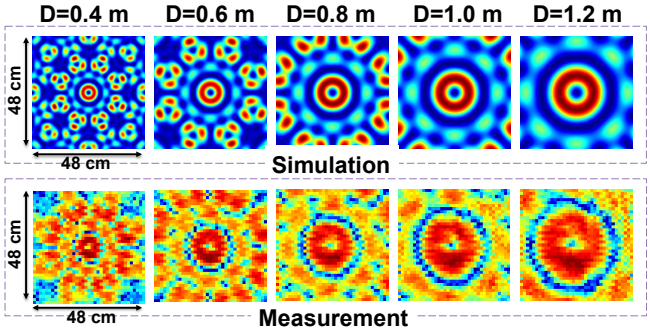

Figure 4. Simulated (top) and measured (bottom) intensity profiles of the generated OAM +1 at different distances after the transmitter. D: distance from the transmitter to the receiver plane.

To measure the transverse phase of the generated OAM beams, a Gaussian beam is employed to interfere with the generated beam through a beam splitter (see Fig. 5(a)). The beam splitter used in the experiment is similar in form to the polka-dot beam splitter used in free space optics. It is fabricated with a printed-circuit board, which has a spatially varying reflective surface. Such a beam splitter has 50% transmission efficiency for a 28 GHz beam incident at a 45o angle relative to the plane of the beam splitter [4,24]. Figures 5(b) and 5(c) show the simulated and measured inference patterns of the generated beam with a Gaussian beam. A clear rotating arm can be seen, indicating that OAM+1 is generated. Note that the scanned area of the interference pattern is 40 cm × 40 cm, which is smaller than the intensity profile. This is because of the size limitation of the beam splitter.

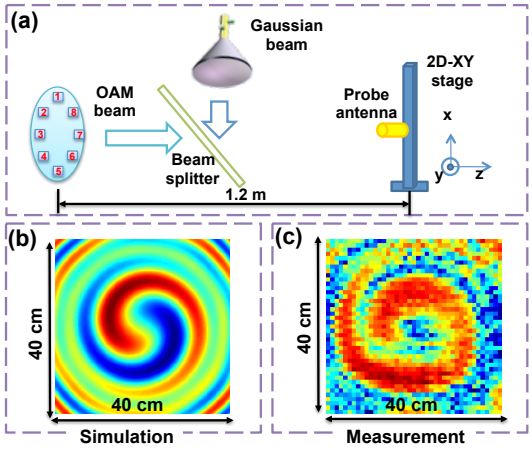

Figure 5. (a) Experimental setup for the interference pattern between the generated OAM+1 beam and a Gaussian beam. (b) Simulated and (c) measured interference pattern.

IV. Steering of the Generated OAM+1 Beam

The OAM+1 beam generation using a circular antenna array has been introduced. We further demonstrate steering of the generated OAM+1 beam. Figure 6 shows the relative phase delays among the antennas. The phase delays among the antennas could be separated into two different components: (i) a spatial phase delay for the OAM generation, which is 0, π/8, π/4, 3π/8, π/2, 5π/8, 3π/4, 7π/8 for the eight antennas (Fig. 6 (a)); and (ii) a tilted wave front for beam steering in y-axis (x and y axis are defined in Fig. 3(a)), where the relative phase delays increase as the position of the antenna goes from left to right in x direction (Fig. 6 (b)). Since the beam steering is designed in y direction, in terms of beam steering, antennas #1 and #5 always have the same phase delay regardless of the steering angle due to them having the same x coordinate. This is the same case for antennas #2 and #4, and antennas #6 and #8. The phase delays in Fig. 6 (c) are the sum-up of the phase delays in Figs. 6(a,b), which correspond to the simultaneously OAM generation and beam steering, respectively.

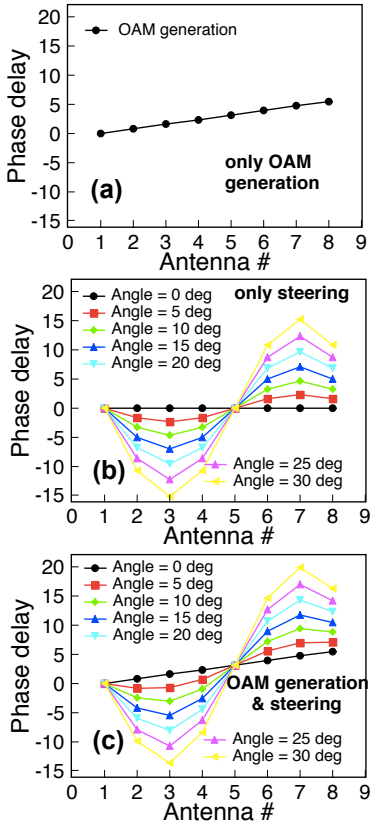

Figure 6. Relative phased delays among the antennas for (a) only OAM+1 generation, (b) only beam steering, and (c) both OAM generation and beam steering. Note that the phase delays in (c) are the sum-up of the phase delays in (a) and (b). Antenna # refers to the i_{th} antenna, where i = 1, 2, 3, ..., 8.

In order to measure the quality and steering angle of the steered OAM beam, we put the 2D stage 1.2 m after the circular antenna array (Fig. 7 (a)) to scan the intensity profile of the steered OAM beam. In this figure, the beam is propagating at an angle relative to the z-axis, while the transverse intensity is measured in a plane perpendicular to the z-axis. The intensity profiles of the steered OAM beams are shown in Fig. 8. A steering angle of as large as 30° is achieved. For large steering angles, we observe significant distortion to the OAM beam. We believe that this is caused by the following reasons: (i) The scanning plane is not perpendicular to the beam propagation axis for the steering angles > 0°, therefore, the measured intensity profile may contain distortion due to the angle misalignment (e.g., the 2D stage is scanning on a tilted plane). Note that if a proper estimation of beam propagation direction, clear OAM intensity patterns (or even interfence

patterns) could be reconstruct. For example, one part of the beam may propagate a little bit more distance than the other part (as shown in Fig. 7 (b)). (ii) Larger steering angle would require larger phase delays among antennas. For the fixed number of the antennas in the experiment, the phase delay resolution in terms of beam steering is relatively lower for larger steering angle.

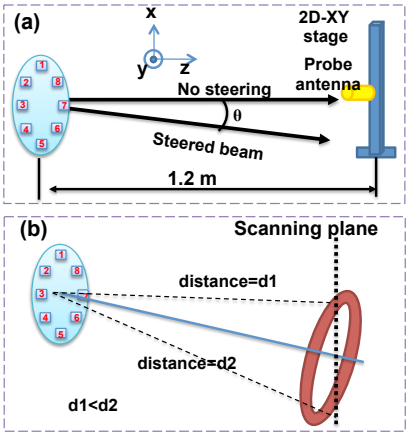

Figure 7. (a) Designed scheme of scanning the intensity profiles for the steered OAM beams. (b) Postion of the steered beam and the scanning plane.

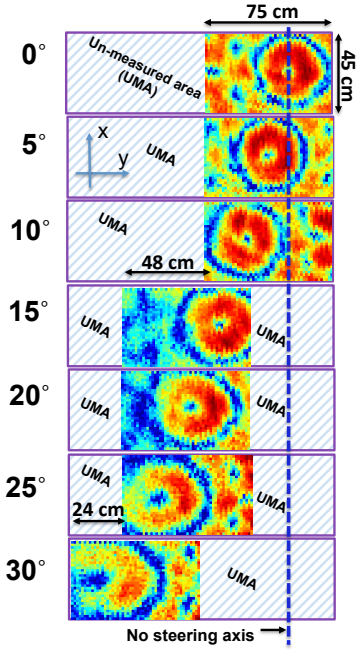

Figure 8. Scanned intensity profiles of the steered OAM beams with the designed steering angle ranging from 0° to 30°. Stripes show un-measured area.

The comparison between the designed and measured steering angle is shown in Fig. 9. When the steering angle is small, the design and the measurement are in good agreement. However, the difference increases when the steering angle is increased. This is due to the lower phase delay resolution for a arger steering angle, which causes a decreased steering accuracy. At steeper steering angles, large measurement deviations are caused by the inability to correctly determine the center of the beam as ring-shaped intensity is measured as an oval-shaped intensity due to the tilt angle (Fig. 8).

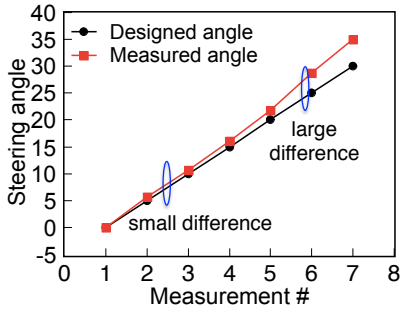

Figure 9. The designed/measured steering angle under different realizations.

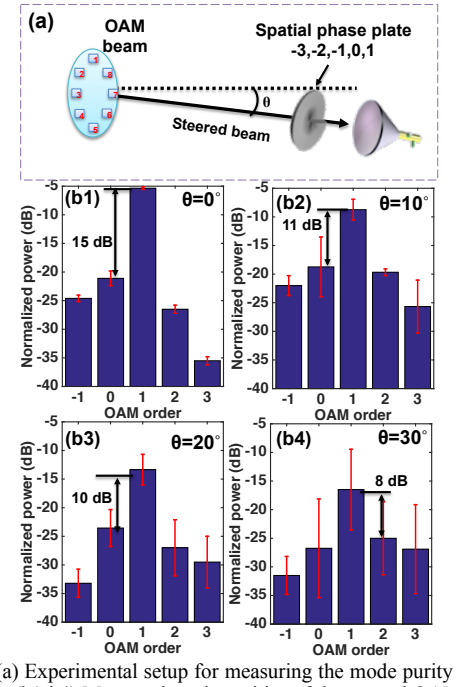

Figure 10. (a) Experimental setup for measuring the mode purity of the steered OAM beam. (b1-b4) Measured mode purities of the steered OAM beams when the steering angle is 0°, 10°, 20°, and 30°, respectively. Error bars in the figures indicate the accuracy of the measurement.

OAM mode purity is an important metric that indicates the quality of an OAM beam. OAM mode purity is defined as the power distribution over the neighboring OAM modes and itself when a specific OAM beam is transmitted. The less the power is leaked to the neighbors, the purer the OAM mode is. Note that for a theoretically OAM modes are pure and therefore their inner product with other mode results in zero power due to the orthogonality. Figure 10 (a) shows the experimental setup for OAM mode purity measurement. A spiral phase plate (SPP) with the OAM order of -l is placed on the propagation axis to convert the power on OAM +l component of the steered OAM beam (if any) into a Gaussian-like beam. A horn antenna, which theoretically only couples a Gaussian-like beam, is followed to collect down-converted beam. This approach could be considered as the decomposition of a beam into OAM basis. The SPP is defined by its thickness which varies azimuthally according to $h(\phi) = (\phi/2\pi)\ell\lambda/(n-1)$, acquiring a maximum thickness difference of $\Delta h = \ell\lambda/(n-1)$ (φ is the azimuthal angle, n is the refractive index of the plate material, λ is the wavelength of the millimeter-wave) [4, 19]. When the SPP order is l, the power received by the horn antenna indicates the power of OAM-l component in the steered beam.

We vary l among +1, 0, -1, -2, and -3. The measured OAM mode purities with different steering angles are shown in Fig. 10 (b). When the steering angle is 0° (no steering), the power differences between OAM+1 and its neighbors are larger than 15 dB. However, as the steering angle increases, such power differences decrease. This is due to the decreased phase delay resolution caused by the larger steering angle. It also affects the phase delays for OAM beam generation since the phase delays for beam steering and OAM generation are controlled by the same delay line array. Note that in the experiment, the SPP and horn antenna are supposed to be perpendicular to the propagation axis of the steered beam but they may not be perfectly aligned since the beam propagation axis is not perfectly measured. Therefore, the results shown in Fig. 10 (b1-b4) are based on the average of multiple measurements. As indicated by the error bar, the measurement for large steering angle suffers large deviation.

V. Parameters Design of the Circular Array Antenna

The use of a circular antenna array for the steering and generation of OAM beams have been demonstrated. Here, the effects of the circular array's parameters (e.g. distance from antennas to the array center, number of the antennas) to the quality of the generated OAM beams are discussed.

A. The generation of OAM +2

In order to demonstrate the generation of OAM +2 using the designed circular antenna array, the relative phase delays for the 8 antennas are tuned to be 0, $\pi/4$, $\pi/2$, $3\pi/4$, π, $5\pi/4$, $3\pi/2$, and $7\pi/4$, respectively. The beam's intensity profile and its interference pattern with a Gaussian beam are scanned by the designed 2D stage that is placed 1.2 m away from the transmitter. Figure 11 shows the simulated and measured intensity profile and interference pattern. The intensity profile of the generated OAM+2 is a ring shape with several glitches. Moreover, the interference pattern of OAM+2 is not as clear as that of OAM+1. Therefore, when using the same number of antennas for OAM generation, higher order OAM beams may suffer more distortions.

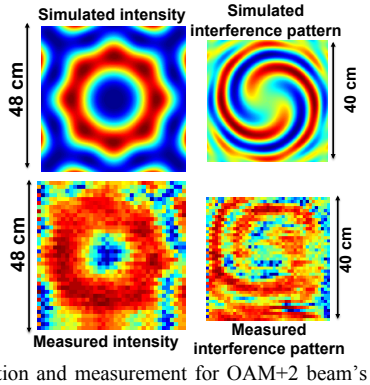

Figure 11. Simulation and measurement for OAM+2 beam's intensity profile and its interference pattern with a Gaussian beam using designed antenna array.

B. Generation of "OAM +1" beam using a 4-antenna array

The generation of "OAM+1" beam using a 4-antenna array is also demonstrated, in which the relative phase delays among the 4 antennas are tuned to be 0, $\pi/2$, π, and $3\pi/2$, respectively. The simulation and measurement for the intensity profile of the generated beam is scanned 1.2 m away from the transmitter as shown in Figure 12. No obvious ring shape is observed, which indicates that in order to generate the same order of OAM beams, increasing the antenna number may help to improve the quality of the generated beam.

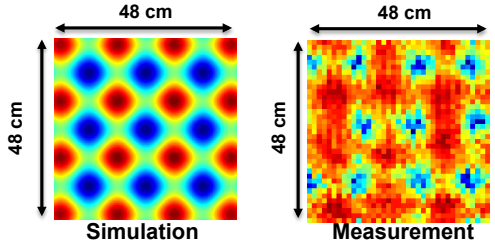

Figure 12. Simulated and measured intensity profile for the generated "OAM+1" using a 4-antenna array.

C. The distance from antennas to the array center

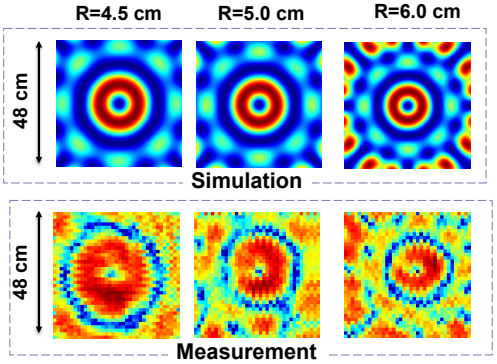

Figure 13. Simulated and measured intensity profiles of the generated OAM+1 with R= 4.5 cm, 5.0 cm and 6.0 cm, respectively. R: the distance from the antennas to the array center.

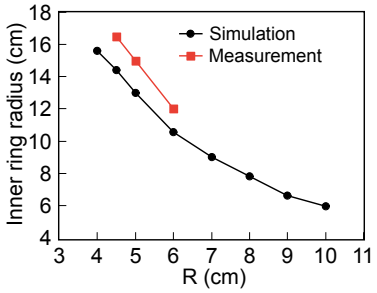

Figure 14. Compararion between the simulation and measurement for the most inner ring radius of the generated OAM beam under different distances from the antenna to the array center.

Previously, the distance from antennas to the array center (i.e., R in Fig. 3(a)) is fixed to be 4.5 cm. Here, this distance is varied from 4.5 cm to 5.0 cm and 6.0 cm. The antenna number is fixed to be 8 and the antenna's radius is fixed to be 2.1 mm. Figure 13 shows the simulated and measured intensity profiles of the generated OAM+1 at a plane 1.2 m away from the transmitter for R=4.5 cm, 5.0 cm and 6.0 cm, respectively. The simulation and measurement agree with each other. Increasing distance from the antennas to the array center allows the reduction of the beam size at the receiver. Taking the innermost ring as an example, its size as a function of the distance from the antennas to the array center (e.g., R) is shown in Fig. 14. If the beam generated by the antenna array is considered as a single beam, the distance from the antennas to the array center seems to be proportional to the beam waist of

the single beam, where increasing its beam waist at the transmitter leads to the reduction of the beam divergence.

VI. Discussions

The following points are also worth mentioning:

- The eight antennas used in our experiment are not completely identical to each other. When the antennas are equalized as is done in phase array radar system, better results would be expected.
- The tunable delay lines in the experiment have insertion loss and we observed fluctuations in the insertion loss while tuning the delay. Therefore, the power of different branches is not perfectly equalized. Better results are expected if all branches are equalized in power.
- We only demonstrate the largest angle that the generated OAM beam could be steered using the custom-designed antenna array. The resolution of the steering angle (the minimum angle that could be achieved) is not demonstrated. Generally, the resolution of the steering angle is determined by the resolution of the phase delays. It is expected that if the phase delay resolution is increased, the steering angle resolution could also be improved.
- The use of circular antenna array for OAM beam generation and steering is demonstrated at 28 GHz. Note that this approach could also be applied to other frequencies.

VII. Summeray

The generation and steering of beams carrying orbital angular momentum using a custom-designed circular antenna array has been experimentally demonstrated at the frequency of 28 GHz. As large as a 30° steering angle has been achieved with the OAM power leaked to the neighboring mode less than -8 dB. The effects of the antenna numbers, the distance from antennas to the array center, and the order of the OAM beams to the quality of the generated beam have been investigated. The results indicate that: (i) increasing the number of the antennas allows for the increase of the generated mode purity and the power on the inner rings of the beam; (ii) increasing the distance from the antennas to the array center would cause smaller divergence to the generated OAM beams.

Acknowledgment

We thank Donald R. Wiggins from the University of Southern California for the discussion and help on designing the breadboard for holding the antennas. We acknowledge supports of Intel Labs University Research Office, NSF ECCS-1509965 and MRI-1126732, and NxGen Parteners.

References

[1] R. W. Lucky, "The precious radio spectrum [Reflections]," IEEE Spectrum, vol. 38, no. 9, 90-90, 2001.

[2] G. Gibson, J. Courtial, and M. J. Padgett, et. al, "Free-space information transfer using light beams carrying orbital angular momentum," Optics Express, vol. 12, no. 22, pp. 5448-5456, 2004.

[3] J. Wang, J.-Y. Yang, and I. M. Fazal, et. al, "Terabit free-space data transmission employing orbital angular momentum multiplexing," Nature Photonics, vol. 6, no. 7, pp. 488-496, 2012.

[4] Y. Yan, G. Xie, and Martin P. J. Lavery, et. al, "High-capacity millimetre-wave communications with orbital angular momentum multiplexing," Nature communications, vol. 5, 2014.

[5] P J. Winzer, "Making spatial multiplexing a reality," Nature Photonics, vol. 8, no. 5, 345-348, 2014.

[6] B. Thidé, H. Then, and J. Sjöholm, et. al, "Utilization of photon orbital angular momentum in the low-frequency radio domain," Physical review letters, vol. 99, no. 8, p. 087701, 2007.

[7] F. E. Mahmouli, and S. D. Walker, "4-Gbps uncompressed video transmission over a 60-GHz orbital angular momentum wireless channel," IEEE Wireless Communications Letters, vol. 2, no. 2, pp. 223-226, 2013.

[8] F. Tamburini, E. Mari, and A. Sponselli, et. al, "Encoding many channels on the same frequency through radio vorticity: first experimental test," New Journal of Physics, vol. 14, p. 033001 2012.

[9] F. Tamburini, E. Mari, and Bo Thidé, et. al, "Experimental verification of photon angular momentum and vorticity with radio techniques," Applied Physics Letters, vol. 99, no. 20, p. 204102, 2011.

[10] I. Djordjevic, "Deep-space and near-Earth optical communications by coded orbital angular momentum (OAM) modulation," Optics Express, vol. 19, pp. 14277-14289, 2011.

[11] M. Tamagnone, C. Craeye, and J. Perruisseau-Carrier, "Comment on 'Encoding many channels on the same frequency through radio vorticity: first experimental test', New Journal Physics, vol. 14, p. 118001, 2012.

[12] O. Edfors, and A. J. Johansson, "Is orbital angular momentum (OAM) based radio communication an unexploited area?" IEEE Transcation on Antennas and Propagation, vol. 60, no. 2, pp. 1126-1131, 2012.

[13] G. A. Turnbull, D. A. Robertson, and G. M. Smith, et. al, "The generation of free-space Laguerre-Gaussian modes at millimetre-wave frequencies by use of a spiral phaseplate," Optics communications, vol. 127, no. 4, pp. 183-188, 1996.

[14] S. M. Mohammadi, L. K. Daldorff, and J. E. Bergman, et. al, "Orbital angular momentum in radio—a system study," IEEE transactions on Antennas and Propagation, vol. 58, no. 2, pp. 565-572, 2010.

[15] Y. Ren, L. Long, and G. Xie, et al., "Experimental demonstration of 16 Gbit/s millimeter-wave communications using MIMO processing of 2 OAM modes on each of two transmitter/receiver antenna apertures," in Proc. of IEEE Global Communication, Austin, 2014.

[16] G. Molina-Terriza, J. P. Torres, and L. Torner, "Twisted photons," Nature Physics, vol. 3, no. 5, pp. 305-310, 2007.

[17] A. Yao, and M. J. Padgett, "Orbital angular momentum: origins, behavior and applications," Advances in Optics and Photonics, vol. 3, no. 2, pp. 161-204, 2011.

[18] L. Cheng, W. Hong and Z. Hao, "Generation of electromagnetic waves with arbitrary orbital angular momentum modes," Scientific Reports, vol. 4, 2014.

[19] A. Tennant and B. Allen, "Generation of OAM radio waves using circular time-switched array antenna," Electronics letters, vol. 48, no. 21, pp. 1365-1366, 2012.

[20] Z. Li, Y. Ohashi, and K. Kasai, "A dual-channel wireless communication system by multiplexing twisted radio wave," in Proc. IEEE European Microwave Conference (EuMC), pp. 235-238, 2014.

[21] F. Spinello, E. Mari, and M. Oldoni, et. al, "Experimental near field OAM-based communication with circular patch array," arXiv preprint arXiv:1507.06889, 2015.

[22] G. Xie, L. Li, and Y. Ren, et. al, "Performance metrics and design considerations for a free-space optical orbital-angular-momentum–multiplexed communication link," Optica, vol. 2, no. 4, pp. 357-365, 2015.

[23] D. K. Nguyen, O. Pascal, and J. Sokoloff, et. al, "Antenna gain and link budget for waves carrying orbital angular momentum (OAM)," arXiv preprint arXiv:1504.00289, 2015.

[24] N. Yu, P. Genevet, and M. A. Kats, et al., "Light propagation with phase discontinuities: generalized laws of reflection and refraction," Science, vol. 334, no. 6054, pp. 333-337, 2011.